JSR Publications

Available Online

J. Sci. Res. **2** (2), 214-220 (2010)

JOURNAL OF SCIENTIFIC RESEARCH

www.banglajol.info/index.php/JSR

Tetracene Based OTFT with Nd_2O_3-dielectric Layer

R. Sarma[1], D. Saikia[1*], P. Saikia[2], and P. K. Saikia[2]

[1]Thin Film Laboratory, Department of Physics, J B College, Jorhat, Assam, India

[2]Dibrugarh University, Dibrugarh, Assam, India

Received 8 January 2010, accepted in final revised form 20 March 2010

Abstract

Tetracene thin film transistors with rare earth oxide (Nd_2O_3) as gate dielectric is reported in this work. Rare earth oxide with high dielectric constant and low leakage current improve the performance of the organic thin film transistors (OTFTs). The fabricated tetracene OTFTs have shown good output characteristics with mobility $0.93x10^{-4}$ $cm^2/V.s$, ON-OFF ratio $3.3x10^2$, sub-threshold swing 0.06 V/decade and hole concentration $8.74x10^{17}$ cm^{-3}.

Keywords: Organic thin film transistors; Tetracene; Rare earth oxide; Trap density.

© 2010 JSR Publications. ISSN: 2070-0237 (Print); 2070-0245 (Online). All rights reserved.

DOI: 10.3329/jsr.v2i2.4094 J. Sci. Res. **2** (2), 214-220 (2010)

1. Introduction

Organic thin film transistors (OTFT) are currently the subject of substantial international research, with much potential in commercial applications such as flexible display panel [1, 2], chemical sensors [3, 4], electronic paper [5]. Compared to traditional silicon devices, they have low production costs; much of the processing can be performed at or near room temperature; and the techniques involved tend to be simpler than for silicon. Compared with a conventional non-organic transistor, the OTFT can be constructed at a lower temperature. In addition, the organic thin film transistor involves simpler manufacturing processes [4] that do not require certain high precision technique and equipment. In this regard, the OTFT are of great potential and interest for further development. Although the organic thin film transistor has the advantages as described above, there are still some bottlenecks choking such as low carrier mobility and high driving voltage.

The organic materials that have been used as active semiconductor materials in OTFTs include both oligomers [6, 7] and polymers [8**]**. An organic semiconductor is an organic

[*]*Corresponding author*: dipk.saik@gmail.com

compound that possesses similar properties to inorganic semiconductors with hole and electron conduction layer and a band gap [9]. Organic semiconductors differ from other organic materials in that the molecules have л conjugate bonds which allow electrons to move via л-electron cloud overlaps.

A schematic diagram of the OTFT configuration is shown in Fig. 1. OTFT of short chain (oligomers) organic semiconductors can be prepared by vacuum evaporation method while OTFT long chain (polymers) molecules can be prepared by spin coating method.

Rare earth oxides such as La_2O_3, Pr_6O_{11}, Nd_2O_3 were reported [10] for next generation high-k gate insulator, and they showed excellent electrical properties such as high dielectric constant and small equivalent oxide thickness (EOT) with low leakage current density. We have already successfully fabricated tetracene OTFTs with La_2O_3 gate insulator [11] and pentacene OTFTs with Pr_6O_{11} insulator [12]. In this work we have used Nd_2O_3 as gate insulator (Figs. 2).

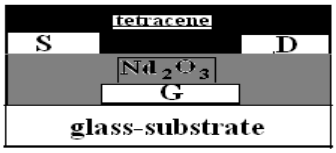

Fig. 1. A schematic illustration of a tetracene-OTFT configuration.

Fig. 2. Photograph of the fabricated tetracene OTFTs.

2. Experimental Details

In this present work, the TFTs were prepared by multiple pump down (MPD) method. Using this method, each film of the TFT will be laid down on an insulating substrate, which is glass in our case, using proper masks. After each deposition, the vacuum is broken and the entire TFT is grown in step by step by using the masks of desired shape.

We first deposited metal (Al) gate electrode of thickness 1120 Å on a glass substrate, above which a dielectric layer of Nd_2O_3 of thickness1160 Å is deposited. In the next step source drain electrodes of aluminum (of thickness 1200 Å) having a channel length 50μm (using wire grill) were deposited, finally a tetracene semiconductor layer of thickness 440 Å was depositions at vacuum better than 8×10^{-6} torr.

3. Results and Discussions

In Fig. 3 we have plotted variation of drain current (I_D) with drain voltage (V_D) at various gate voltage. In the figure we also compare experimental values with the theoretical values (calculated with Eq. 1) and it is seen that they almost agree with one another which established the reliability of the fabricated device.

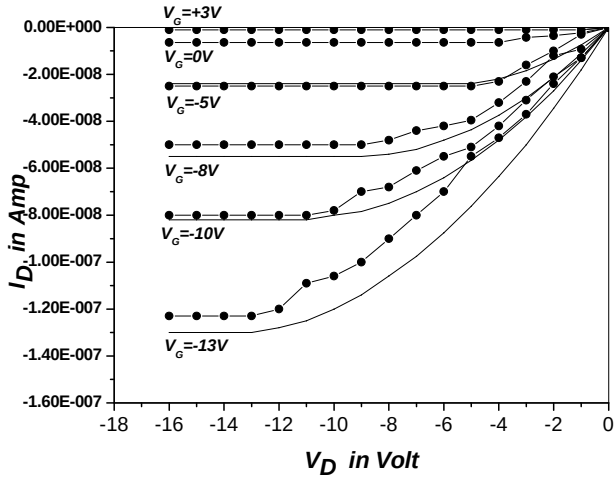

Fig. 3. Variation I_D *vs* V_D (dotted lines indicate experimental variations while smooth lines indicate theoretical variations).

The increase in current with the negative gate voltage indicates field-effect-induced hole conduction, which is the expected behaviour for tetracene. The theoretical equation for drain current (I_D) is [13]:

$$I_D = \frac{w}{L} \mu c_i \left(V_G - V_T - \frac{V_D}{2} \right) V_D \tag{1}$$

where w is the channel width, L is channel length, C_i is the capacitance per unit area of the gate insulator, V_T is the threshold voltage and μ is the mobility.

In Fig. 4 we have plotted the variation of saturated drain current $(I_{Dsat})^{1/2}$ *vs.* gate voltage V_G for the high negative gate voltage the variation is almost linear while for the low negative voltage the plot shows unusual results. The slope of the linear reason of the plot $(I_{Dsat})^{1/2}$ vs. V_G gives the mobility $\boldsymbol{\mu}$ and the extrapolation of the linear region of the plot to the V_G axis gives the threshold voltage V_T [13]. The observed threshold voltage is 1.2V. The positive threshold voltage for p-channel devices may indicate the presence of unwanted p-dopant in the organic layer, thus a positive V_G is needed to switch off the device [14]. The calculated mobility value with Eq.2 is 0.93×10^{-4} $cm^2/V.s$.

$$I_{Dsat} = \frac{w}{2L} \mu c_i \left(V_G - V_T \right)^2 \tag{2}$$

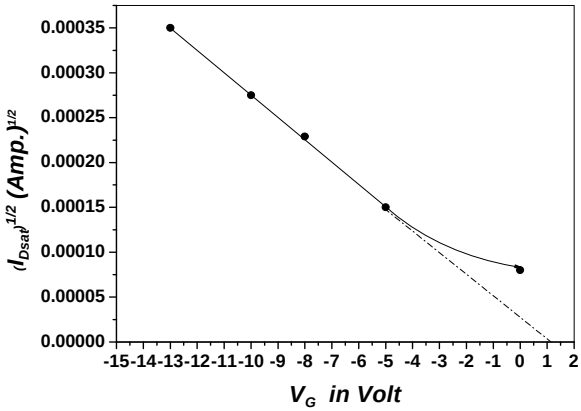

Fig. 4. Plot of $(I_{Dsat})^{1/2}$ vs V_G.

The sub-threshold swing is calculated from the slope of the graph shown in Fig. 5 using the relation [15]:

$$s = \left(\frac{d\left(\log I_D\right)}{dV_G} \right)^{-1} \tag{3}$$

The calculated value of sub-threshold swing is 0.06 V/decade. Normalizing [16] this value to the capacitance of the dielectric gives 30 VnF/decade.cm^2. These values are comparable to what is found for the best pentacene TFTs (15-80 VnF/decade.cm^2) [17, 18].

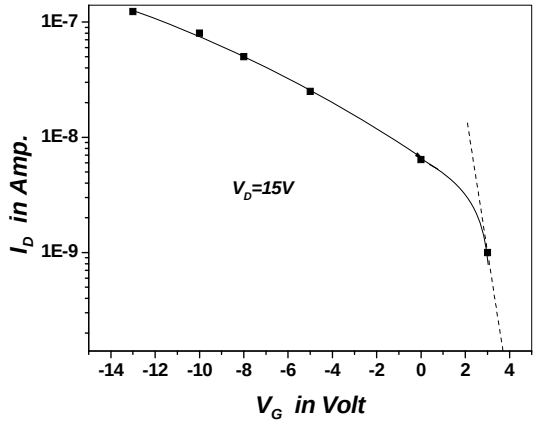

Fig. 5. $\text{Log}_{10}(I_D)$ vs. V_G characteristics for the tetracene TFT at V_D=15V.

The maximum number of interface traps (or trap density) present is estimated using the following relation assuming that the densities of the deep bulk states and interface states are independent of energy [19]:

$$N_{ss}^{\max} = \left\{ \frac{s(\log e)}{KT/q} - 1 \right\} \frac{C_i}{q} \tag{4}$$

The estimated value is $0.074 \times 10^{11} eV^{-1}$ cm^{-2}. The channel conductivity σ is estimated from the plot of I_D vs. V_D graph at zero gate voltage. The ON-OFF ratio is estimated from the following relation [13]:

$$\frac{I_{ON}}{I_{OFF}} = \frac{c_i \mu (V_G - V_T)^2}{\sigma d V_D} \tag{5}$$

The estimated value of on-off ratio is 3.3×10^2.

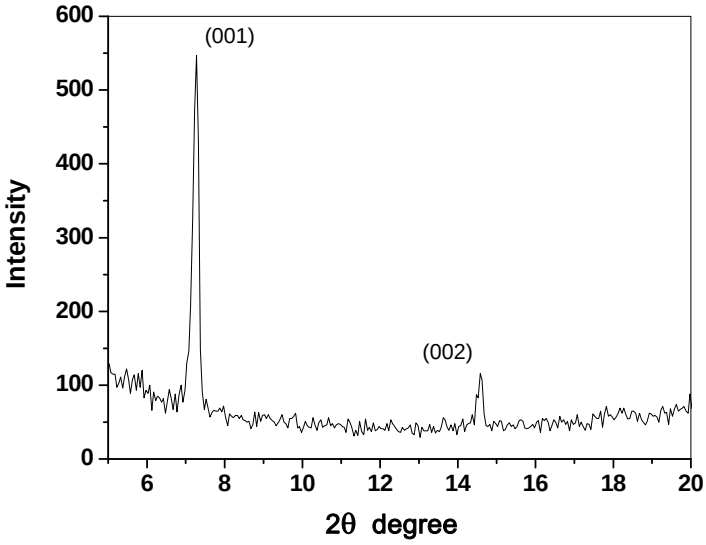

Fig. 6. XRD pattern of the tetracene thin film deposited on glass substrate.

The XRD of the tetracene film is shown in Fig. 6. The Bragg's peaks at (001) and at (002) indicate that the tetracene molecules are packed parallel to each other in a nearly vertical direction where *c*-axis of the tetracene molecules are aligned perpendicular to the substrate. The report established that the tetracene films are polycrystalline in nature and is composed of linear chain of identical crystallites.

The various values of the parameter used and evaluated are tabulated in Table 1.

Table 1. The various parameters used and evaluated.

Channel width (w)	0.14 cm
Channel length (L)	0.005 cm
Capacitance per unit area (c_i)	0.005 F/m^2
Channel thickness (d)	440 Å
Threshold voltage (V_T)	1.2 V
Channel Mobility (μ)	0.93×10^{-4} m^2/V.s
Channel Conductivity (σ)	1.3×10^{-5} Ω^{-1} cm^{-1}
Sub threshold swing (s)	0.06 V/decade
I_{ON} / I_{OFF}	3.3×10^{2}
Hole concentration (N_P)	8.74×0^{17} cm^{-3}
Maximum numbers of interface traps present (N_{ss}^{max})	0.74×10^{11} eV^{-1} cm^{-2}

4. Conclusions

The fabricated OTFTs have well defined *I-V* characteristics. ON-OFF ratio of the OTFTs better than $3.3x10^2$. The normalizing value of sub-threshold swing to the capacitance of the dielectric is 30VnF/decade.cm^2, which is comparable to what is found for the best pentacene TFTs (15-80VnF/decade.cm^2) [17, 18]. These results can be considered as satisfying for tetracene OTFT with Al-electrodes. The values can be further improved using Au-source drain electrode which offers less contact resistance than Al-electrodes.

Acknowledgement

The authors acknowledge the University Grant Commission, New Delhi, India for financial support under major research project program.

References

1. M. Mizukami, N. Hirohata, T. Iseki, K. Ohtawara, T. Tada, S. Yagyu, T. Abe, T. Suzuki, Y. Fujisaki, Y. Inoue, S. Tokito, and T. Kurita, IEEE Electron Device Lett. **27** (4), 249 (2006). doi:10.1109/LED.2006.870413
2. S. Ono and Y. Kobayahi, Jpn. J. Appl. Phys. **43** (12), 7947 (2004). doi:10.1143/JJAP.43.7947
3. F. Liao, C. Chen, and V. Subramanian, Sensors and Actuators B: Chemical **107**, 849 (2005). doi:10.1016/j.snb.2004.12.026
4. M. Halik, H. Klauk, U. Zschieschang, G. Schmid, C. Dehm, M. Schütz, S. Maisch, F. Effenberger, M. Brunnbauer, and F. Stellacci, Nature **431**, 963(2004). doi:10.1038/nature02987
5. S. H. Han, S. M. Cho, J. H. Kim, J. W. Choi, and J. Jang, Appl. Phys. Lett. **89**, 093504 (2006). doi:10.1063/1.2338526
6. A. L. Briseno, S. C. B. Mannsfeld, M. M. Ling, S. Liu, R. J. Tseng, C. Reese, M. E. Roberts, Y. Yang, and F. Sacuto, Phys. Rev. B **70**, 081309(R) (2004).

8. H. Yan, Z. Chen, Y. Zheng, C. Newman, J. R. Quinn, F. Dötz, M. Kastler, and A. Facchetti, Nature **457**, 679 (2009). doi:10.1038/nature07727
9. G. Horowitz, Advanced Materials **2**, 287 (1990). doi:10.1002/adma.19900020604
10. H. J. Osten**,** J. P. Liu, P. Gaworzewski, E. Bugiel, and P. Zaumseil, IEDM Tech. Dig. 653 (2000). doi:10.1103/PhysRevB.70.081309
11. R. Sarma and D. Saikia, Indian J. Pure & Appl. Phys. **47**, 876 (2009).
12 R. Sarma, D. Saikia, and B. Barua, Organic Thin Film Transistor with Pr_6O_{11}-dielectric layer (poster presentation- 42), *In*: Indo-Russian Workshop on Nanotechnology and Laser Induced Plasma Proceedings (IRNANO-2009).
13. B. C. Shekar, J. Lee, and Shi.-W. Rhee, Korean J. Chem. Eng. **21**, 267 (2004). doi:10.1007/BF02705409
14. N. Koch, Chem Phys Chem, **8**, 1438 (2007). doi:10.1002/cphc.200700177
15. J. H. Seo, J.-H. Kwon, S.-Il Shin, K.-S. Suh, and B.-K. Ju, Semicond. Sci. Technol. **22**, 1039 (2007). doi:10.1088/0268-1242/22/9/011
16. R. W. I. de Boer, T. M. Kalpwijk, and A. F. Morpurgo, Appl. Phys. Lett. **83**, 4345 (2003). doi:10.1063/1.1629144
17. D. J. Gundlach, J. A. Nichols, L. Zhou, and T. N. Jackson, Appl. Phys. Lett, **80,** 2925 (2002). doi:10.1063/1.1471378
18. Y. Y. Lin, D. J. Gundlach, S. F Nelson, and T. N Jackson, IEEE Trans. Electron Devices **44**, 1325 (1997). doi:10.1109/16.605476
19. A. Rollend, J. Richard , J. P Kleider, and D. Mencaraglia, J. Electrochem. Soc. **140**, 3679 (1993). doi:10.1149/1.2221149